

Femoral curvature variability in modern humans using three-dimensional quadric surface fitting

Tara Chapman^{1,2} · Victor Sholukha^{2,3} · Patrick Semal¹ · Stéphane Louryan^{2,4} · Marcel Rooze² · Serge Van Sint Jan²

Received: 7 November 2014 / Accepted: 23 May 2015 / Published online: 4 June 2015
© Springer-Verlag France 2015

Abstract

Introduction This study analysed femoral curvature in a population from Belgium in conjunction with other morphological characteristics by the use of three-dimensional (3D) quadric surfaces (QS) modelled from the bone surface.

Methods 3D models were created from computed tomography data of 75 femoral modern human bones. Anatomical landmarks (ALs) were palpated in specific bony areas of the femur (shaft, condyles, neck and head). QS were then created from the surface vertices which enclose these ALs. The diaphyseal shaft was divided into five QS shapes to analyse curvature in different parts of the shaft.

Results Femoral bending differs in different parts of the diaphyseal shaft. The greatest degree of curvature was found in the distal shaft (mean 4.5° range 0.2°–10°) followed by the proximal (mean 4.4° range 1.5°–10.2°), proximal intermediate (mean 3.7° range 0.9°–7.9°) and distal intermediate (mean 1.8° range 0.2°–5.6°) shaft sections. The proximal and distal angles were significantly more bowed than the intermediate proximal and the intermediate distal angle. There was no significant difference

between the proximal and distal angle. No significant correlations were found between morphological characteristics and femoral curvature. An extremely large variability of femoral curvature with several bones displaying very high or low degrees of femoral curvature was also found.

Conclusion 3D QS fitting enables the creation of accurate models which can discriminate between different patterns in similar curvatures and demonstrates there is a clear difference between curvature in different parts of the shaft.

Keywords Femur · Quadric surface · Curvature · Bone palpation

Introduction

Anterior femoral curvature has previously been recognised as a distinct human morphological trait. Earlier studies have demonstrated that there seems to be no straightforward relationship between femoral curvature and a single other morphological trait, but rather that curvature of the femur is complex and is likely to come from a number of factors [22, 24, 28]. Femoral curvature is present in the developing embryo [18]. Development of this curvature may be caused by factors such as the intrinsic growth pattern of the femur or extrinsic factors such as muscular tension and mechanical forces acting within the knee [17]. The femur is a weight bearing bone continuously subject to mechanical loading which causes the form and structure of the bones to change [29]. The interaction of physical and morphological properties (such as length, weight, density, femoral neck angle, femoral neck anteversion angle, etc.) must therefore also be of importance in determining the degree of femoral curvature [24, 28, 30].

✉ Tara Chapman
tchapman@ulb.ac.be; tara.chapman@naturalsciences.be

¹ Operational Direction 'Earth and History of Life', Royal Belgian Institute of Natural Sciences, Brussels, Belgium

² Laboratory of Anatomy, Biomechanics and Organogenesis, Faculty of Medicine, Université Libre de Bruxelles, Brussels, Belgium

³ Department of Applied Mathematics, Peter the Great St. Petersburg Polytechnic University, St. Petersburg, Russia

⁴ Department of Radiology, ULB Erasme Hospital, Brussels, Belgium

There have been many attempts to understand femoral curvature in conjunction with other biological [2, 8, 10–12, 15, 22, 24, 25, 28, 30, 31], morphological [2, 7, 12, 22, 25] and cultural [11] factors. To date, however, the extent of human variability and the function of sagittal femoral curvature still remains largely unknown. Recent studies have mainly been in the context of medical interventions such as how femoral curvature could influence outcome of total knee arthroplasty (TKA) and compatibility with intramedullary nails (which are metal rods inserted into the femur to treat breakages) [3, 5, 16, 25, 30, 31].

Numerous studies state that femoral curvature may be related to population differences [8, 10–12, 15, 24, 25, 28, 30, 31]. Studies on Asian populations report that current navigation systems in TKA and intramedullary nail size and shape are not well designed for Asian populations due to differences in the femoral shape and sagittal femoral curvature of these populations [3, 5, 16, 25, 30, 31]. The correct alignment of the lower limb is correlated with clinical success in TKA. The majority of studies focus on the correct alignment of the coronal plane and sagittal alignment has thus far been largely overlooked. However, clinical studies [5, 21, 30] state that the sagittal plane should be considered in TKA as large variances in sagittal femoral curvature could result in negative patient outcome such as the development of degenerative arthritis in the knee, limited extension and the piercing of the distal anterior femoral cortex [5, 21, 30]. This is similarly the case with the use of intramedullary nails.

The majority of femoral intramedullary nails currently available have a radius of curvature (ROC) of between 150 and 300 cm [10, 12, 13]. However, studies on both intra and inter populations have shown that the ROC of most intramedullary nails does not adequately match the femoral curvature of most adult femurs [2, 10, 20]. This mismatch of nail size with femoral shape and size causes complications, such as distal femur anterior cortex perforation and hip, thigh and knee pain (which has been reported in up to 75–90 % of patients after surgery [2, 10, 19, 20, 31]).

A significant drawback of the ROC is that it only gives the overall curvature of the femur and not whether curvature differs in different parts of the femur. The analysis of the effect of sagittal femoral curvature in medical interventions has seen a growth of studies using radiographs and three-dimensional (3D) modelling to analyse femoral curvature [2, 4, 25]. Femoral shape is extremely complex and thus 3D models need to be simplified in order to analyse bone morphology. The quadric surface (QS) approach has previously been adopted in the study on femoral curvature by Yehyawit et al. [30] who modelled the femoral shaft in three sections using ellipsoids [30]. In this new study, bone morphology was simplified by modelling quadric surfaces

(ellipsoids, one-sheet hyperboloids and two-sheet hyperboloids). Anatomical landmarks were palpated in specific bony areas of the femur (femoral shaft, condyles, neck and head). Quadric surfaces were then created from surface vertices which enclose these landmarks [23]. The use of QS shapes to analyse the diaphyseal shaft enabled the shaft to be divided into five sections to analyse degree of curvature in different parts of the femoral shaft.

Morphological factors such as femoral head and neck anatomy and the position of the condyles have been cited as possible correlations with femoral curvature [30]. The position of the femoral head and several femoral neck angles has also previously been shown to be extremely variable [23]. These are all factors which may ultimately be related and could better help predict femoral curvature. The aim of this study was to examine femoral curvature in a population from Belgium in different sections of the femoral shaft and to analyse these differences in conjunction with other morphological characteristics. An important factor in the development of the method was to develop a protocol which could accurately and efficiently analyse femoral bone morphology and curvature, which would enable the application to be used in clinics [23] and fundamental research.

Materials and methods

Data were collected from computed tomography data (CT) of 75 femoral (39 right + 36 left) anatomically modern human bones available from the ULB bone repository (10 pairs of bones were from fresh frozen donors; 2 pairs of bones from two volunteers who underwent medical imaging for clinical purposes not related to bone disorders; the remainder were from dry bones). Fresh frozen specimens and volunteers were of Belgian origin. Dry specimens used in this study were from the Body Donation programme at the Université Libre de Bruxelles, Brussels, Belgium (note that donors were anonymous to these authors for ethical reasons; the head of the Body Donation programme has stated that all donors to the program are Belgian). Sex and age for the dry bones were not known. Bones appeared normal and did not show any signs of joint disorders although many of the bones appeared to be of an advanced age. The two volunteers did not complain of any osteo-articular disorders. 3D reconstruction of bones was performed in the software programme Amira, bone models were built in the global reference system of the CT system and stored using a standard format (i.e. vrml) and further imported into the lhpFusionBox software (which is a musculo-skeletal data processing software developed at the Université Libre de Bruxelles).

All bone models were further processed by virtual palpation to determine the spatial locations of three ALs: lateral epicondyle (FLE), medial epicondyle (FME) and greater trochanter (FTC) [27] (Fig. 1). The three palpated ALs were then used in a semi-automatic process performed in MATLAB© to add further landmark clouds on each femur using an affine registration based on a template of landmarks to accurately measure femoral bending and other morphological factors (Fig. 1), [23].

Following the above semi-automatic process—each bone was manually checked by trained anatomists to ensure that ALs and AL clouds were located correctly. AL clouds were then used as a base with which to identify

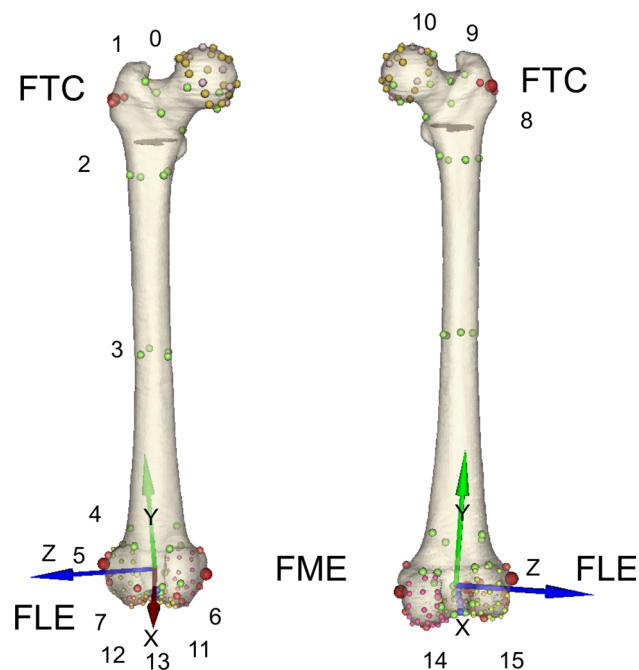


Fig. 1 All anatomical features digitised in this study (illustrated on a 3D model of a femur; the model has been rendered transparent to allow better visualisation of the local frame attached to the bone) with palpated ALs and corresponding anatomical reference frame (ARF). Three landmarks (FTC, FME, FLE) were palpated which enabled an ARF (X-, Y- and Z-axes indicated on femur) to be created. The Y-axis (in green) passes from the mid-point of (FLE, FME) to FTC. The X-axis (in red) is oriented anteriorly and perpendicular to the plane containing FLE, FME and FTC. The Z-axis (in blue) is orthogonal to the X- and Y-axes. Each bone vertex and AL was then transferred from the global imaging frame to the origin of the femoral anatomical reference frame. Landmark clouds were placed in specific areas via a semi-automatic process performed in MATLAB. All clouds were then manually checked to ensure accuracy. Clouds 0–7 = ALs for cutting planes for specific areas of vertexes selection (green). Cloud 8 = ALs for registration for femur (red); Cloud 9 = femoral head (lilac); Cloud 10 = femoral head (light brown); Cloud 11 = patella surface medial condyle (mustard); Cloud 12 = patella surface lateral condyle (orange); Cloud 13 = middle of patella surface (blue); Cloud 14 = tibial surface of medial condyle (coral); Cloud 15 = tibial surface of lateral condyle (yellow) (color figure online)

surface vertices in nine anatomical segments (femoral head, femoral neck, five diaphysis segments, lateral and medial condyles). Once vertices were identified in each area this enabled the bone to be split into several specific areas (Fig. 2). Bone area splitting was performed in MATLAB using a semi-automated method to pre-process each bone from the database. The bone template was then transformed to each database bone by heterogeneous weighted scaling using the available ALs. All left bones were mirrored to right bones to increase the population size [23].

QS data fitting

The landmark clouds on the nine areas-of-interest (Fig. 2) were then used to approximate joint surface by primitive geometrical shapes. Approximate primitive shapes, similar to Yehyawi et al. [30] were used as it is too complex to use the surface of the bone for analysis. The method was such that the approximated primitive object should uniquely define a closed area corresponding to the 3D shape vertices and enclose the available palpated landmarks as accurately as possible. Surface vertices relating to each specific area were selected using the cutting planes evaluated from landmarks previously virtually palpated (Fig. 1) (see Sholukha et al. [23] for further details of the method).

To estimate the accuracy of QS data fitting error, the shortest distance was evaluated between the QS surface and the bone surface vertices. The method was taken from Eberly [9] and full technical details are available from Sholukha et al. [23].

Geometric shapes and landmark configurations were then used to analyse the size and orientation of femoral head, neck and condyles. Surface square, volume, size and

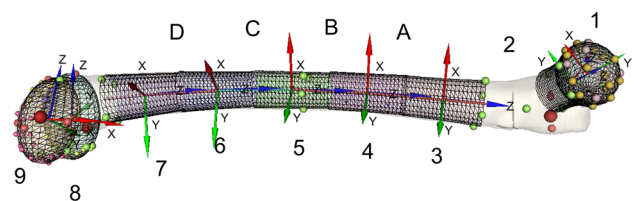


Fig. 2 Quadric surfaces used in the study. Nine anatomical segments of the femur were fitted by quadric surfaces (indicated by wireframes) 1. femoral head; 2. femoral neck; 3. proximal diaphysis; 4. proximal intermediate diaphysis; 5. centre of diaphysis; 6. distal intermediate diaphysis; 7. distal diaphysis; 8. lateral condyle; 9. medial condyle. **a** Proximal angle; **b** intermediate proximal angle **c** intermediate distal angle; **d** distal angle. All bones were aligned in the same LCS (Fig. 1). Individual quadric surfaces were orientated using a QS shape (represented by a wireframe) visible at the centre of each QS (X-, Y- and Z-axes of local coordinate systems are indicated on the femur and are color-coded red, green and blue for the X-, Y- and Z-axes, respectively). The Z-axis for each of the individual diaphysis segments was orientated along the femoral shaft to enable analysis of femoral sagittal curvature (color figure online)

orientation of the femoral head, length of the femur, segments of the diaphyseal shaft and condyles were measured. Femoral curvature was estimated as the sum of the angles between the longitudinal axes (Z-axes *in blue*) of the 5 diaphysis segments in the sagittal plane (Fig. 2). This enabled the angle of the curvature to be measured and the degree of bending at different locations of the femoral shaft to be analysed.

Previously palpated ALs were further used to analyse the following measurements and angles: head–trochanter–condyle (htc) angle which is an approximation of the cervico-diaphyseal angle, condylar hip angle, sagittal mechanical axis and estimation of length, anteversion angle, intercondylar angle (Fig. 3). The sagittal mechanical axis was defined as the line between the centre of the femoral head and midpoint between FME centre of the medial epicondyle and FLE of the centre of the lateral epicondyle (Fig. 3). Following Chung et al. [5] the angle between the sagittal mechanical axis (Fig. 3) and the Z-axis of each of the diaphyseal segments (Fig. 2) were analysed for correlation with sagittal femoral bending. Alignment of the hip–knee–ankle (hka) angle is mainly determined by the distal femoral valgus condylar hip angle and the proximal tibial–plateau varus (plateau–ankle angle) as the angle between the joint surfaces (condylar–plateau) is relatively constant [6]. The condylar hip angle is the angle of the femoral condylar tangent with respect to the femoral mechanical axis and demonstrates whether the knee is varus positive or

varus negative [6]. To determine if the hka angle is related to sagittal femoral curvature, we analysed the condylar hip angle (as it was not possible to analyse the plateau–ankle angle). The Angle CH was expressed as the degree of deviation from 90° (negative for varus and positive for valgus).

Correlations were performed between femoral curvature and other morphological variables. Data were tested for normality and appropriate statistical tests were used.

Results

QS surfaces were fitted automatically according to the surface vertices. The mean QS fitting error for each of the segments analysed demonstrates that small errors were found in the fitting of QS data (Table 1). The highest error was found in the distal bending of the shaft. The average error was 1.0 mm and the maximum error was found to be 2.5 mm. The shape of the femoral head and medial and lateral condyles were all found to be close to ellipsoids. The shape of the majority of the diaphyseal shaft segments were close to one-sheet hyperboloids. The femoral neck was shown to have the greatest variability in shape and varied from an ellipsoid (with long Z semi-axis) to a one-sheet hyperboloid shape.

There was found to be an extremely large degree of variability for the overall curvature (8.7°–24.0°) (Table 2). The highest degree of femoral curvature was found in the distal shaft of the femur (Angle D, 4.5° range 0.2°–10°). The second biggest degree of femoral curvature was found in the proximal shaft (Angle A, 4.4° range 1.5°–10.2°), followed by the proximal intermediate proximal shaft (Angle B, 3.7° range 0.9°–7.9°). The least amount of curvature was found in the intermediate distal shaft (Angle C, 1.8° range 0.2°–5.6°). The degree of curvature between adjacent segments also enabled the analysis of the radius of curvature (ROC) in different parts of the shaft. Femoral curvature in this study was estimated as the angle (or sum of angles for the whole diaphyseal shaft) between the Z-axes of the five diaphysis segments in the sagittal plane. To obtain ROC, the length of the Z-axes in two adjacent diaphyseal segments or the sum of the length of all five Z-axes in the diaphyseal shaft was added (see Fig. 2) and the following calculations were made:

Angle between two adjacent segments or sum of all angles $\times \pi/180$ gives the radian.

Then length of the Z-axis of two adjacent segments or sum of the five Z-axes/radian = radius of curvature (ROC) (Table 2).

There was also found to be a wide range of human variability for each of the angles and variables measured (Table 3).

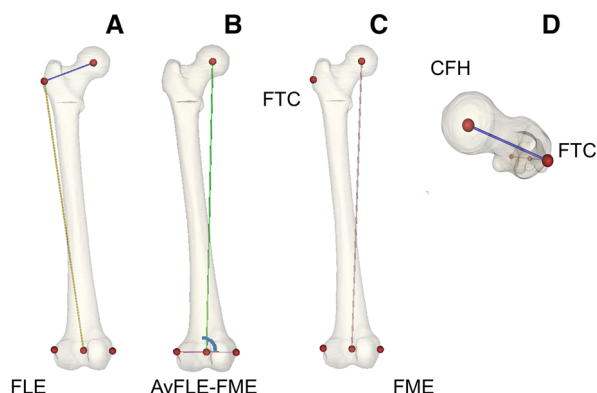


Fig. 3 Calculation of angles and measurements. Lateral epicondyle (FLE), medial epicondyle (FME) and greater trochanter (FTC) were the original palpated landmarks. The centre of the femoral head (CFH) was defined as the centre of the ellipsoid (Fig. 2) which enclosed all palpated landmarks in this area. Similarly, the centre of the lateral condyle (CLC) and the centre of the medial condyle (CMC) were the centre of the ellipsoids of the condyles (Fig. 2). AvFLE-FME was the average between FLE and FME. **a** Head–trochanter–condyle angle (i.e., angle between the line AvFLE-FME to FTC and the line FTC to CFH or angle between *blue* and *yellow* lines); **b**, **c** sagittal mechanical axis of the femur and estimation of length; **d** femoral neck anteversion angle or cervico-bicondylar angle (color figure online)

Table 1 Quadric Surface data fitting error in mm

	Mean error	SD error	Maximum error	Minimum error	Estimated QS types		
					As ellipsoid	As 1-sheet hyperboloid	As 2-sheet hyperboloid
Femoral head	0.5	0.5	1.3	0.2	75	0	0
Femoral neck	1.2	1.0	2.0	0.7	32	35	8
Proximal diaphyseal shaft	0.5	0.4	1.4	0.3	7	68	0
Proximal intermediate diaphyseal shaft	0.6	0.5	1.5	0.4	6	69	0
Centre diaphyseal shaft	0.8	0.5	1.5	0.3	33	42	0
Distal intermediate diaphyseal shaft	0.6	0.5	1	0.3	10	63	2
Distal diaphyseal shaft	1.0	0.8	2.5	0.5	3	71	1
Lateral condyle	1.1	0.9	1.8	0.7	75	0	0
Medial condyle	1.2	0.9	2.2	0.6	75	0	0

Last three columns indicate the amount of particular QS type in the area of interest

Table 2 Curvature of the femur with mean, median, maximum, minimum degree and radius of curvature (ROC)

	No of specimens	Angle A°	Angle B°	Angle C°	Angle D°	Sum of all °
Mean degree°	75	4.4°	3.7°	1.8°	4.5°	14.4°
Standard dev°		1.7°	1.2°	1.1°	1.8°	3.1°
Median°		4.2°	3.7°	1.7°	4.7°	14.0°
Minimum°		1.5°	0.9°	0.2°	0.2°	8.7°
Maximum°		10.2°	7.9°	5.6°	10.0°	24°
Mean ROC (cm)	75	91	103	310	138	123
Standard dev		40	47	314	293	29
Median		80	94	204	80	119
Minimum		29	37	66	42	60
Maximum		230	356	2093	2030	202

Angles (in degrees) A–D between the various shaft segments are represented in Fig. 2

Table 3 Human variation in selected variables

	Surface square (cm ²)	Volume (cm ³)	Femoral head radius (mm)	Head-trochanter-condyle angle (°)	Condylar hip angle (°)	Femoral neck anteversion angle (°)	Intercondylar angle (°)	Estimation of length (mm)
Human mean	623.3	507.0	22.9	126.4	1.9	−4.9	37.1	395.2
Standard dev	74.5	92.7	1.7	7.7	1.5	9.2	6.2	27.2
Median	622.6	508.6	23.1	127.3	1.8	−5.8	36.3	393.0
Minimum	475.1	333.6	19.0	108.3	1.3	−18.6	25.1	339.5
Maximum	769.4	706.1	26.7	145.5	6.4	24.4	54.1	468.8

Statistical tests

Appropriate statistical tests were used. All outliers were checked and bones were found to be without fracture or abnormalities and there were no errors in the 3D data and landmarks. Spearman's rank correlation coefficient was performed to determine the relationship between femoral curvature and specific individual variables. There was a

medium, positive correlation between the sum of femoral curvature overall and Angle A (0.500) and Angle D (0.619) and a weak positive correlation between the sum of femoral curvature overall and Angle B (0.341) and Angle C (0.322) (Table 4).

A Wilcoxon signed rank test was performed to analyse differences between curvatures in different parts of the shaft. There were highly significant differences between

both distal (Angle D) curvature and intermediate proximal (Angle B) curvature ($z = -3.570$, $p = < 0.000$) and intermediate distal (Angle C) curvature ($z = -6.954$, $p = < 0.000$). There were highly significant differences between both proximal (Angle A) curvature and intermediate proximal (Angle B) curvature ($z = -2.793$, $p = 0.005$) and intermediate distal (Angle C) curvature ($z = -7.245$, $p = < 0.000$). There was no significant difference between the proximal (Angle A) curvature and distal (Angle D) curvature ($z = -7.87$, $p = 0.431$). There was also a highly significant difference between the intermediate proximal (Angle B) curvature and intermediate distal (Angle C) curvature ($z = 6.585$, $p = < 0.000$).

Surface square, volume, radius of femoral head and other angles of the femoral neck and head were not correlated with femoral curvature either in the different sections or overall (Table 4). There was a weak positive correlation with the estimation of length (0.352) (Table 4). The X, Y and Z position of the centre of the femoral head and neck and condyles in relation to the diaphyseal shaft were also analysed and no correlations were found. The condylar hip angle was not correlated with femoral curvature and the angles between the sagittal mechanical axis (Fig. 3) and the Z-axis of each of the diaphyseal segments (Fig. 2) were not correlated with sagittal femoral bending. A Mann–Whitney U test was also conducted to compare differences in bending in the left and right femurs. There

was no difference between left and right femurs in all angles: proximal angle ($U = 737$, $p = 0.0.684$); intermediate proximal angle ($U = 417$, $p = 0.450$); intermediate distal angle ($U = 401$, $p = 0.172$); distal angle ($U = 401$, $p = 0.172$); overall angle ($U = 435$, $p = 0.443$).

Discussion

The developed method of analysing bone by Quadric Surfaces (QS) has demonstrated that it is a useful tool in order to analyse the complexity of femoral curvature in conjunction with other morphological characteristics of the bone. The use of landmarks to delineate areas enables accurate modelling of the diaphysis and epiphyses of the femur by the use of surface vertexes [23]. The small amounts of errors from QS surfaces demonstrate that this is a viable method to model femoral morphology (Table 1). The femoral head and condyles of all femurs were modelled as ellipsoids (Table 1). The majority of the diaphyseal shaft segments were correctly estimated using one-sheet hyperboloids (with the exception of the centre of the diaphyseal shaft which was also demonstrated to have an ellipsoid shape). The femoral neck had the greatest shape variability (Table 1). The study also enabled measurements to be automatically analysed in exactly the same way through the use of the local coordinate system (LCS) where all bones are placed in exactly the same position (Figs. 1, 3, 4).

The study has shown that femoral bending in this study differs in different parts of the diaphyseal shaft. The greatest degree of curvature was found in the distal shaft (Angle D, 4.5° range 0.2° – 10°) closely followed by the proximal shaft (Angle A, 4.4° range 1.5° – 10.2°), with less curvature found in the proximal intermediate (Angle B, 3.7° range 0.9° – 7.9°) and distal intermediate (Angle C, 1.8° range 0.2° – 5.6°) sections of the femoral shaft (Fig. 2; Table 2). The proximal angle and the distal angle were significantly more bowed than the intermediate proximal angle and the intermediate distal angle and there was no significant difference between the proximal and distal angle. There was also a medium, positive correlation between the sagittal bending angle overall and both the proximal and distal angle (Table 4). This study enabled the shape of the femur from a Belgian population to be accurately characterised. The result of this study is in line with other studies using varying methods, that have reported that curvature is not consistent throughout the shaft [4, 25, 30, 31].

Yehyawi et al. [30] in a similar study examined the femoral shaft of American patients by modelling the shaft in three ellipsoids. They found less mean curvature overall (8.78° range $<2^\circ$ – 14.99°), with the largest curvature in the

Table 4 An example of some correlation coefficients between sum of curvature overall and other variables

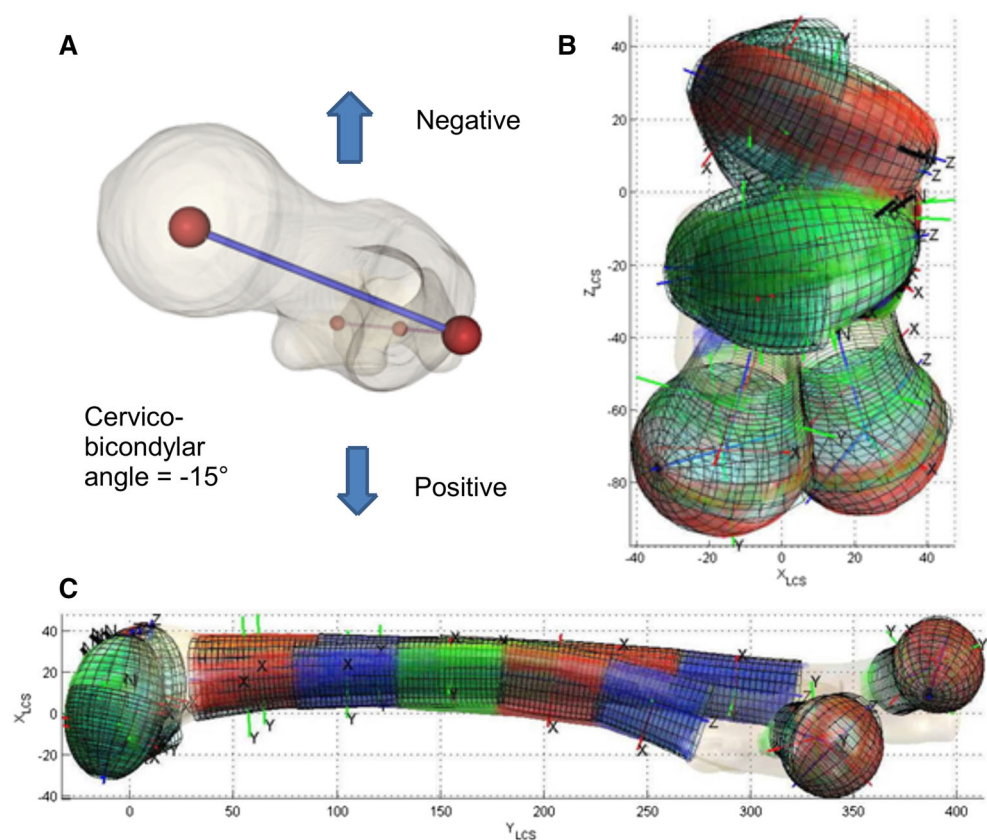
Variable	Spearman's rank correlation coefficient	Significance (2 tailed)
Volume	0.121	0.301
Surface square	0.136	0.245
Angle A	0.500	0.000
Angle B	0.341	0.003
Angle C	0.322	0.005
Angle D	0.619	0.000
Head radius	0.090	0.443
Head–trochanter–condyle angle	−0.36	0.764
Anteversion/bicondylar angle	−0.46	0.705
Intercondylar angle	−0.132	0.263
Condylar hip angle	0.241	0.037
Estimation of length/sagittal mechanical axis	0.352	0.002
ROC 1	0.552	0.000
ROC 2	0.384	0.001
ROC 3	0.362	0.001
ROC 4	0.636	0.000
ROC overall	0.954	0.000

proximal shaft (5.25° range $<1^\circ$ – 9.99°), followed by the distal shaft (3.28° range $<1^\circ$ – 6.99°), with the least amount of curvature found in the centre (0.25° range $<0.10^\circ$ – $>1.60^\circ$). This is further in contrast to numerous studies on the Asian population that have used varying methods and report that the greatest degree of curvature is found in the distal part of the shaft [4, 16, 25, 31]. These studies seem to show that population differences do exist. However, studies on populations tend to give an overall average statistic—and there is an extremely large variability of femoral curvature (Table 2). Several bones presented extreme degrees of femoral curvature (Table 2). The proximal and distal curvatures were statistically similar on average (Table 2); however, there were several femurs which had much greater proximal than distal bending and vice versa.

A large variation in femoral curvature has been found with other studies although comparisons are difficult as methodologies differ. Seo et al. [21] analysed sagittal bending in an Asian population by analysing the angle between the longitudinal axis of the proximal and distal femur (using the medullary canal as a reference). They found a similar femoral overall bending to this study in that mean femoral bending was (13.9° : range 6.2° – 24.5°) in comparison to femoral curvature in our study (14.4° : range 8.7° – 24.0°). Twiesselmann [26] previously found a large

variation in a study on a Belgian population which analysed the highest maximum point of curvature from 394 femurs: chord length (406 range 332–492); subtense (17.2 range 3–34). The radius of curvature (ROC) of the femur is also widely variable with reported ranges from 48 to 567 cm and means of 90–120 cm [1, 4, 10, 13] (different populations also have different averages, i.e. Chantapanich et al. [4] reported a mean of 90 cm with arrange of 48–163 cm for a Thai population). The method used in this study to analyse the degree of femoral curvature also enabled us to obtain the ROC. This study found a ROC of 123 cm range 60–202 cm, which is in line with current studies and similar to Egol et al. [10] (Table 2). As the majority of femoral intramedullary nails currently available have a ROC of between 150 and 300 cm [10, 12] this means that current nail designs are much straighter than the average human femur, regardless of population [2, 10, 19, 20, 31]. ROC in different parts of the shaft was also shown to be widely variable (Angle A, 91 cm range 29–230 cm; Angle B, 103 cm range 37–356 cm; Angle C, 310 cm range 66–2093 cm; Angle D, 138 cm range 42–2030 cm) (Table 2). It is therefore important that accurate individual morphology of the sagittal femoral curvature is known to help improve the healthcare and recovery of patients who require medical intervention on the femur, whether through TKA or intramedullary nailing.

Fig. 4 Variability in sagittal bending, femoral neck anteversion angle and size. The femoral neck anteversion angle was found to be the greatest variable with a wide variability in the femoral head position. **a** An example of femoral neck anteversion angle and how this was measured; **b**, **c** examples of variability in femoral neck anteversion angle (b), length and sagittal bending in local coordinate system



Based on the initial findings of this study it could be hypothesised that the average femoral shape in this population from Belgium, where there is no statistical difference between the proximal and distal curvature is different from the average shape of the Asian femur where there is a much greater bending in the distal part of the femur. This study also differs from that of the population from America which has demonstrated a greater bending in the proximal area than in the distal part of the shaft.

This study found that there was no correlation between the condylar hip angle and sagittal femoral bending nor was there a correlation between the sagittal mechanical axis and the Z-axis of each of the diaphyseal segments (Figs. 2, 3). Chung et al. [5] analysed the sagittal mechanical axes with distal femoral axes and found significant differences between the two which were related to sagittal femoral curvature. Seo et al. [21] attempted to define the mechanical axis of the femur in the sagittal plane during TKA and found that sagittal bowing of the femur was correlated with the axis of the distal femoral anterior axis but not with the palpable sagittal axis. This may be related to the fact that there is greater sagittal bending in the distal section of the femur in the Asian population although further studies are needed.

The study further demonstrated that there is a wide range of femoral variability in other morphological factors such as head–trochanter condyle angle, anteversion angle, intercondylar angle, position and size of femoral condyles and condylar hip angle (Table 3). The large variability of these morphological characteristics is seemingly not correlated with the large variability of femoral curvature. There were no correlations between different morphological factors such as the position and orientation of the femoral neck, head and condyles as suggested by Yehyawit et al. [30]. There was also no correlation between the size of the shaft and size of femoral condyles. This was surprising as we would have expected a relationship between femoral curvature and head position, but this may be linked to the fact that femoral curvature is highly variable. There was a weak positive correlation with the estimation of length (0.352) (Table 4).

In conclusion, this study has demonstrated that 3D QS fitting enables the creation of accurate models which can discriminate between different patterns in similar curvatures and has demonstrated there is a clear difference between curvature in different parts of the shaft. The application of 3D modelling rather than the single measurement of ROC or the highest point of curvature gives a detailed and accurate description of femoral curvature in different parts of the shaft and in conjunction with other morphological characteristics. Knowledge of the precise curvature of the femoral shaft has implications for the outcome of patients following medical interventions such

as use of navigation systems in TKA and the usage and shape of the intramedullary nail. In line with other studies on the femoral curvature of the femur, this study also demonstrates that femoral curvature is extremely complex and important individual variations are present. It suggests that surgical procedures should integrate a careful analysis of compatibility between the shape of the surgical material used (prosthesis, intradiaphyseal material, etc.) and the individual shaft curvature during pre-planning. The method could also be used to study morphological characteristics, including curvature, in other bones such as the radius, humerus and ribs.

Given the lack of correlation found in morphological factors in this study, we suggest that future research on sagittal femoral bending should also look to other cultural and biological factors. De Groot [7] and Shackelford and Trinkaus [22] hypothesised that femoral curvature may be more to do with activity levels. Activities such as walking, running, different types of sport and whether patients are active or inactive should be taken into account when examining femoral curvature to gain a true understanding of activities which may contribute to this curvature. The method used in this study could be applied to study the dimension of the femoral medullary canal in comparison to medullar implants and nails, similar to other authors [2, 12, 14]. The method can further be studied with any statistical parameters such as age, sex and laterality. Sex and age should be taken into account and population differences should be a factor when examining patients due to the large number of studies that find statistical significances in the curvature of the femur between populations [10–12, 15, 24, 25, 28, 30, 31], including this study. It is also important to take into account the large variability within populations and not rely solely on the average which may obscure data and to uncover what is behind differences between different populations, whether they are of a genetic origin [11, 17, 28] as a consequence of urban vs rural living [22], activity levels, [7, 22] or any other factor.

We hope that with a greater sample size (gained through our semi-automatic method) we may be able to uncover more complexity in the future. The method has been developed so that there is the potential that each new patient who visits the hospital for a femoral CT scan could be added to the database if they chose to consent to the study. From this CT scan and only three landmarks we are then able to extract a large quantity of data. The use of an automated template also means that further landmarks can be added to analyse different measurements if required. Each new bone could then be imported into a database which could also contain further patient information (i.e. information such as whether the patients are active or inactive). In this way, a large collection of femoral bones can be collected to analyse whether a greater proportion of

bones yields different results. The alignment of the prosthetic and femoral component following reconstruction of the knee (TKA) is critical to patient outcome following surgery. It would therefore also be interesting to analyse femoral curvature in conjunction with morphological characteristics of the pelvis and tibia of the same individual where a full CT scan of the lower limb was available. The CH angle was not correlated with femoral curvature in this study; however, an examination of all the components of the hip–knee–ankle angle may yield a different result.

Acknowledgments The authors thank Mr. Hakim Bajou (LABO, ULB) for his technical assistance in scanning the bone material. We thank François Euran for his assistance in palpation of landmarks. We thank Bruno Bonnechère for his assistance with statistics. The research was performed as part of a doctorate financed by the Belgian Federal Public Planning Service Science Policy (BELSPO, Action 2).

Conflict of interest The authors declare that they have no conflict of interest.

References

- Bruns W, Bruce M, Prescott G, Maffulli N (2002) Temporal trends in femoral curvature and length in medieval and modern Scotland. *Am J Phys Anthropol* 119(3):224–230. doi:10.1002/ajpa.10113
- Buford WL Jr, Turnbow BJ, Gugala Z, Lindsey RW (2014) Three-dimensional computed tomography-based modeling of sagittal cadaveric femoral bowing and implications for intramedullary nailing. *J Orthop Trauma* 28(1):10–16. doi:10.1097/bot.0000000000000019
- Chang SM, Song DL, Ma Z, Tao YL, Chen WL, Zhang LZ, Wang X (2014) Mismatch of the short straight cephalomedullary nail (PFNA-II) with the anterior bow of the femur in an Asian population. *J Orthop Trauma* 28(1):17–22. doi:10.1097/bot.0000000000000022
- Chantarapanich N, Mahaisavariya B, Siribodhi P, Kriskrai S (2011) Geometric mismatch analysis of retrograde nail in the Asian femur. *Surg Radiol Anat* 33(9):755–761
- Chung BJ, Kang YG, Chang CB, Kim SJ, Kim TK (2009) Differences between sagittal femoral mechanical and distal reference axes should be considered in navigated TKA. *Clin Orthop Relat Res* 467(9):2403–2413. doi:10.1007/s11999-009-0762-5
- Cooke TD, Sled EA, Scudamore RA (2007) Frontal plane knee alignment: a call for standardized measurement. *J Rheumatol* 34(9):1796–1801
- De Groote I (2011) Femoral curvature in Neanderthals and modern humans: a 3D geometric morphometric analysis. *J Hum Evol* 60(5):540–548. doi:10.1016/j.jhevol.2010.09.009
- De Groote I, Lockwood CA, Aiello LC (2010) Technical note: A new method for measuring long bone curvature using 3D landmarks and semi-landmarks. *Am J Phys Anthropol* 119 141(4):658–664. doi:10.1002/ajpa.21225
- Eberly D (2008) Distance from a point to an ellipsoid. (<http://www.geometrictools.com/Documentation/DistancePointEllipseEllipsoid.pdf>). Accessed 15 June 2010
- Egol KA, Chang EY, Cvitkovic J, Kummer FJ, Koval KJ (2004) Mismatch of current intramedullary nails with the anterior bow of the femur. *J Orthop Trauma* 18(7):410–415
- Gilbert BM (1976) Anterior femoral curvature: Its probable basis and utility as a criterion of racial assessment. *Am J Phys Anthropol* 45(3):601–604. doi:10.1002/ajpa.1330450326
- Harma A, Germen B, Karakas H, Elmali N, Inan M (2005) The comparison of femoral curves and curves of contemporary intramedullary nails. *Surg Radiol Anat* 27(6):502–506
- Harper MC, Carson WL (1987) Curvature of the femur and the proximal entry point for an intramedullary rod. *Clin Orthop Relat Res* 220:155–161
- Jacq JJ, Roux C (2003) Geodesic morphometry with applications to 3-D morpho-functional anatomy. *Proc IEEE* 91(10):1680–1698. doi:10.1109/JPROC.2003.817863
- Karakas H, Harma A (2012) Femoral shaft bowing with age: a digital radiological study of anatolian caucasian adults. *Diagn Interv Radiol* 14:29–32
- Lu Z-H, Yu J-K, Chen L-X, Gong X, Wang Y-J, Leung KKM (2012) Computed tomographic measurement of gender differences in bowing of the sagittal femoral shaft in persons older than 50 years. *J Arthroplasty* 27(6):1216–1220. doi:10.1016/j.arth.2011.12.024
- Murray PDF (1936) *Bones. A study of the development and structure of the vertebrate skeleton.* Cambridge University Press, London
- Murray PDF, Selby D (1930) Intrinsic and extrinsic factors in the primary development of the skeleton. *Roux Arch* 122:629–662
- Ostrum RF, Levy MS (2005) Penetration of the distal femoral anterior cortex during intramedullary nailing for subtrochanteric fractures: a report of three cases. *J Orthop Trauma* 19(9):656–660
- Scolaro JA, Endress C, Mehta S (2013) Prevention of cortical breach during placement of an antegrade intramedullary femoral nail. *Orthopedics* 36(9):688–692
- Seo JG, Kim BK, Moon YW, Kim JH, Yoon BH, Ahn TK, Lee DH (2009) Bony landmarks for determining the mechanical axis of the femur in the sagittal plane during total knee arthroplasty. *Clin Orthop Surg* 1(3):128–131. doi:10.4055/cios.2009.1.3.128
- Shackelford LL, Trinkaus E (2002) Late pleistocene human femoral diaphyseal curvature. *Am J Phys Anthropol* 119(118):359–370
- Sholukha V, Chapman T, Salvia P, Moiseev F, Euran F, Rooze M (2010) Femur shape prediction by multiple regression based on quadric surface fitting. *J Biomech* 44(4):712–718. doi:10.1016/j.jbiomech.2010.10.039
- Stewart TD (1962) Anterior femoral curvature: its utility for race identification. *Hum Biol* 34:49–62
- Tang W, Chiu K, Kwan M, Ng T, Yau W (2005) Sagittal bowing of the distal femur in Chinese patients who require total knee arthroplasty. *J Orthop Res* 23(1):41–45
- Twisselmann F (1961) *Le fémur néanderthalien de Fond-de-Forêt (Province de Liège).* *Mém Inst Roy Sci Nat, Belg* 148
- Van Sint Jan S (2007) *Color atlas of skeletal landmark definitions: guidelines for reproducible manual and virtual palpations.* Churchill Livingstone Elsevier, Edinburgh
- Walensky NA (1965) A study of anterior femoral curvature in man. *Anat Rec* 151(4):559–570. doi:10.1002/ar.1091510406
- Wolff J (1986) *The law of bone remodelling (trans: Maquet P, Furlong R).* Springer, New York
- Yehyawi TM, Callaghan JJ, Pedersen DR, O'Rourke MR, Liu SS (2007) Variances in sagittal femoral shaft bowing in patients undergoing TKA. *Clin Orthop Relat Res* 464:99–104
- Zhang S, Zhang K, Wang Y, Feng W, Wang B, Yu B (2013) Using three-dimensional computational modeling to compare the geometrical fitness of two kinds of proximal femoral intramedullary nail for Chinese femur. *Sci World J* 2013:978485. doi:10.1155/2013/9784851